

# Tailoring the Surface Chemistry of Anion Exchange Membranes with Zwitterions: Toward Antifouling RED Membranes

Diego Pintossi, Michel Saakes, Zandrie Borneman, and Kitty Nijmeijer\*

Cite This: *ACS Appl. Mater. Interfaces* 2021, 13, 18348–18357

Read Online

ACCESS |



Metrics &amp; More

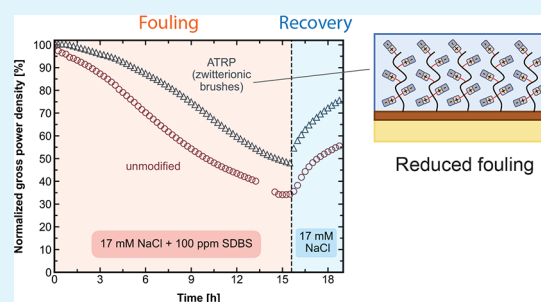


Article Recommendations



Supporting Information

**ABSTRACT:** Fouling is a pressing issue for harvesting salinity gradient energy with reverse electrodialysis (RED). In this work, antifouling membranes were fabricated by surface modification of a commercial anion exchange membrane with zwitterionic layers. Either zwitterionic monomers or zwitterionic brushes were applied on the surface. Zwitterionic monomers were grafted to the surface by deposition of a polydopamine layer followed by an aza-Michael reaction with sulfobetaine. Zwitterionic brushes were grafted on the surface by deposition of polydopamine modified with a surface initiator for subsequent atom transfer radical polymerization to obtain polysulfobetaine. As expected, the zwitterionic layers did increase the membrane hydrophilicity. The antifouling behavior of the membranes in RED was evaluated using artificial river and seawater and sodium dodecylbenzenesulfonate as the model foulant. The zwitterionic monomers are effective in delaying the fouling onset, but the further build-up of the fouling layer is hardly affected, resulting in similar power density losses as for the unmodified membranes. Membranes modified with zwitterionic brushes show a high potential for application in RED as they not only delay the onset of fouling but they also slow down the growth of the fouling layer, thus retaining higher power density outputs.



**KEYWORDS:** reverse electrodialysis, salinity gradient energy, fouling, SDBS, zwitterion, anion exchange membrane

## 1. INTRODUCTION

Salinity gradient energy (SGE) is an energy source derived from the controlled mixing of low and high concentration saltwater streams, e.g., river and seawater, seawater and desalination brines, or thermolytic salt solutions in closed-loop applications.<sup>1–6</sup> SGE has the potential to meet the increasing renewable energy demand without the intermittency issues that plague solar and wind energy. SGE from natural salinity gradients alone has an estimated technical potential of 625 TWh  $y^{-1}$ , which is equal to 3% of the global electricity consumption.<sup>7</sup>

Reverse electrodialysis (RED) is an electro-membrane technology to harvest SGE.<sup>8,9</sup> In RED, cation exchange membranes (CEMs) and anion exchange membranes (AEMs) are stacked alternately to create feedwater compartments where the high and low concentration salt solutions (e.g., 30 and 1 g  $L^{-1}$  NaCl) flow. The salinity gradient across the selective ion exchange membranes results in a potential difference that increases with the number of cell pairs in the RED stack.<sup>10</sup> When an external load is connected to the electrodes to close the circuit, the potential difference can be used to drive an ionic current through the stack. The ionic current can be converted into an electronic current by a suitable redox couple flowing in the electrode compartments.<sup>11</sup>

The potential of RED as a large-scale energy source has been investigated at the laboratory and pilot plant scale,<sup>5,12,13</sup> and

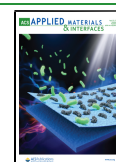
the main obstacles for large-scale RED implementation with natural salinity gradients are fouling and, more in general, membrane costs.<sup>14–16</sup> Fouling is caused by colloids, natural organic matter, multivalent cations and anions, and micro-organisms deteriorating the membrane properties, yielding lower RED power output.<sup>14,17,18</sup> As most foulants are negatively charged, fouling of AEMs is more important than fouling of CEMs. In addition, affinity interactions between the organic contaminants and the polymeric membranes also play a role.<sup>19–26</sup>

To mitigate fouling, stack cleaning protocols and membrane modifications have been thoroughly investigated.<sup>27–29</sup> Periodic feedwater reversal, air sparging, and  $CO_2$  sparging are effective strategies to recuperate fouled membranes and spacers.<sup>27,28</sup> For membrane modification, the desired properties are monovalent-ion selectivity and antifouling functionality to increase the RED power output and the ability to retain it over time.<sup>16,30</sup> Improved resistance to organic fouling is typically obtained by increasing the hydrophilicity of the membrane

Received: February 9, 2021

Accepted: March 30, 2021

Published: April 7, 2021



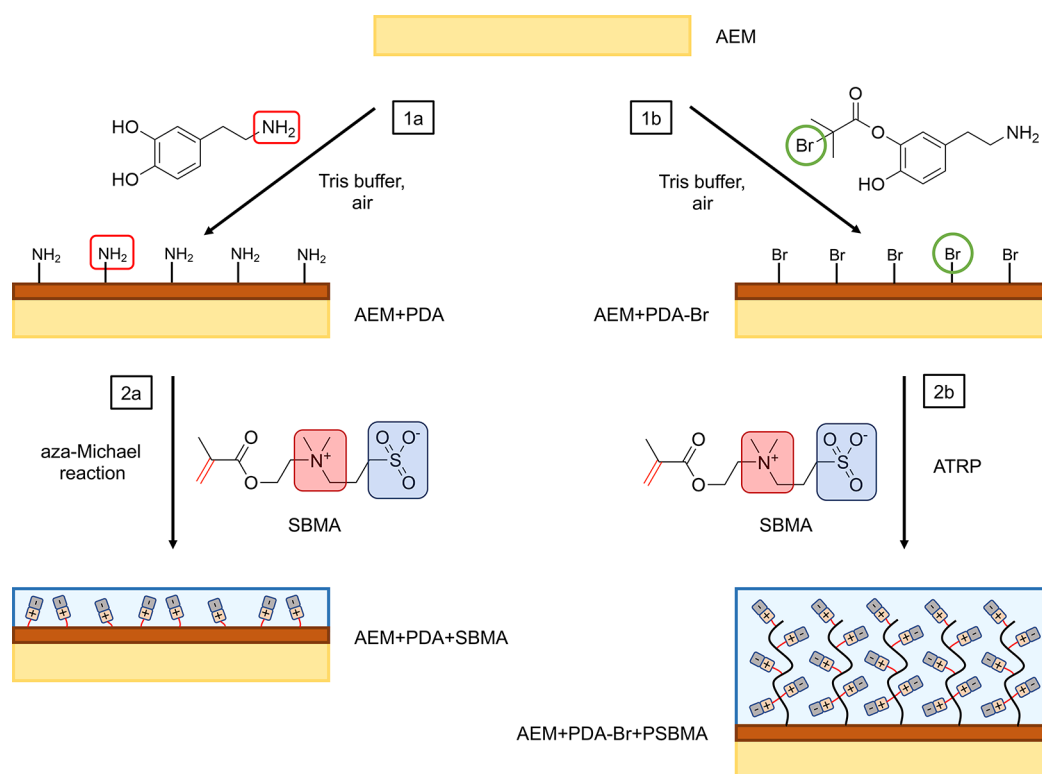


**Figure 1.** Schematic representation of the two surface modification strategies. 1a, Deposition of polydopamine. 2a, Aza-Michael reaction to graft zwitterionic monomers to the membrane surface. 1b, Deposition of polydopamine modified with BiBB. 2b, Atom transfer radical polymerization (ATRP) to graft zwitterionic brushes from the membrane surface.

surface or by deposition of a thin negatively charged layer.<sup>29,31–33</sup>

A promising approach is the use of polydopamine (PDA) to mitigate fouling. Although the application of thick polydopamine layers on the membrane increases its hydrophilicity, thus reducing fouling, and it induces monovalent-ion selectivity by size exclusion, this is done at the expense of decreased membrane charge density and increased membrane resistance.<sup>29,34–38</sup> On the other hand, PDA in the form of a thin layer on a membrane surface is a versatile platform for membrane modification thanks to its functional groups that can undergo further reactions.<sup>39,40</sup>

Zwitterionic coatings are well-known in the biomedical field, where they are used to reduce fouling of surfaces in contact with biological fluids.<sup>41,42</sup> Recently, zwitterionic layers are gaining prominence as effective antifouling layers in the field of water treatment.<sup>43–47</sup> In her review on tackling membrane fouling, Nunes indicated zwitterions grafting as one of the strategies for the fabrication of fouling-resistant membranes.<sup>48</sup> In this regard, Virga et al. recently showed that a zwitterionic top layer is effective in preventive fouling of nanofiltration hollow-fiber membranes during treatment of natural waters.<sup>49</sup> Zwitterionic layers (e.g., polysulfobetaine) are highly hydrophilic due to their ability to retain large hydration shells through hydrogen bonding.<sup>50</sup> Their hydrophilicity combined with a net neutral charge of the zwitterionic layer leads to low interaction with organic pollutants.<sup>44</sup> Liu et al. modified a thin-film-composite membrane first coated with polydopamine with an atom transfer radical polymerization (ATRP) initiator, followed by grafting of polysulfobetaine brushes on the surface and used it in reverse osmosis (RO) for water purification.<sup>40</sup>

Their results show that the zwitterionic brushes impart fouling resistance to the membrane.

Although frequently studied in water purification applications, Ruan et al. provided the only example to date of zwitterionic surface modification of an ion exchange membrane with polysulfobetaine to induce fouling resistance, showing promising results during electro dialysis (ED) of a solution containing sodium dodecylbenzenesulfonate (SDBS) as model foulant, although their investigation spans a limited time scale (2 h) only.<sup>39</sup>

In the present work, we chemically modify the surface of a commercially available AEM with polydopamine bearing zwitterionic functionalities to investigate the benefits of a zwitterionic surface chemistry for fouling resistance in RED. Two different approaches are investigated to assess the antifouling performance of zwitterionic monomers and zwitterionic polymer brushes: (1) AEMs with polydopamine bearing zwitterionic monomer grafts obtained via aza-Michael reaction or (2) AEMs with polydopamine bearing zwitterionic brushes obtained via ATRP. This modification strategy is chosen for its versatility. As a natural adhesive, polydopamine ensures the possibility of modifying any base membrane, irrespective of its chemistry. Additionally, the aza-Michael reaction and ATRP can be used to apply a variety of chemistries on the membrane surface, starting with unsaturated monomers containing the desired functional groups, such as sulfobetaine to obtain a zwitterionic layer. As such, this modification strategy is a platform meant to explore changes to the surface chemistry, and the current work does not intend to show up-scaled applications.

After extensive characterization of the applied layers and the obtained membranes, the membranes are applied in RED to

investigate their fouling behavior in time. The membrane electrical resistance, permselectivity, surface composition and contact angle with water are evaluated at different stages in the modification processes. The fouling resistance of the membranes and their cleaning ability are measured in RED stack experiments where SDBS is added to the river water compartment as a model foulant.

## 2. MATERIALS AND METHODS

**2.1. Materials.** Fujifilm AEM type I membranes (Fujifilm Manufacturing Europe BV, The Netherlands) were used as base membranes for surface modification. The membranes were conditioned at room temperature and stored at 4 °C in 0.1 M NaCl solutions before modification. *N,N*-Dimethylformamide (DMF, 99.99%), absolute ethanol, and 2-propanol (IPA, 99.5%) were used as solvents and purchased from Sigma-Aldrich (The Netherlands). Dopamine hydrochloride (DA), triethylamine (TEA, ≥99.5%), 2-bromoisobutyl bromide (BiBB), tris(hydroxymethyl) aminomethane (Tris), and [2-(methacryloyloxy)ethyl]dimethyl-(3-sulfopropyl)-ammonium hydroxide (known as sulfobetaine methacrylate, SBMA), copper(II) chloride, L-ascorbic acid, and sodium dodecylbenzenesulfonate (SDBS) were also purchased from Sigma-Aldrich. Tris(2-pyridylmethyl)amine (TPMA) was purchased from TCI Chemicals (Belgium). Hydrogen peroxide in 30% solution, copper sulfate pentahydrate, and potassium hexacyanoferrate (both ferri- and ferrocyanide, ≥ 96%) were purchased from VWR Chemicals (Belgium). NaCl (99.5%) was purchased from ESCO (The Netherlands).

**2.2. Surface Modification: Aza-Michael.** **2.2.1. Deposition of Polydopamine.** To improve the homogeneity of the polydopamine (PDA) layers at short deposition times, the procedure used by Zhang et al. was followed.<sup>51</sup> A solution of Tris (700 mg, 5.8 mmol, pH 8.5) and copper sulfate pentahydrate (250 mg, 1 mmol) in 200 mL of milli-Q water was prepared. Then, 407 μL of 30% hydrogen peroxide solution (3.9 mmol) was added to the solution right before deposition. To obtain unmodified polydopamine layers (Figure 1, step 1a), a solution of 2 g dopamine hydrochloride in 200 mL milli-Q water (Merck Millipore, Germany) was prepared. A pristine membrane (11 × 11 cm<sup>2</sup>) was clamped at the bottom of the reactor (Figure S1 in the Supporting Information, open area: 8 × 8 cm<sup>2</sup>). The Tris solution was added in the reactor, quickly followed by 50 mL of polydopamine solution. The reactor was placed on a shaking plate (60 rpm) for 1 h after ensuring adequate mixing of the two solutions. Compressed air was flowing over the solution to ensure oxygen availability inside the reactor was not limited. After modification, the membrane was rinsed in demineralized water and stored in 0.1 M NaCl at 4 °C. The membrane obtained after polydopamine deposition is named AEM+PDA in the following.

**2.2.2. Aza-Michael Reaction.** The procedure for membrane modification with aza-Michael reaction was used as presented by Ruan et al. (Figure 1, step 2a, and Figure S2 in the Supporting Information).<sup>39</sup> Briefly, the membrane modified with polydopamine was immersed in 660 mL of water, 130 mL of absolute ethanol, 5 mL of TEA (acid neutralizer and catalyst for the aza-Michael reaction<sup>52</sup>), and 21 g of SBMA in a round-bottom flask. The solution was heated to 55 °C in an oil bath and gently stirred for 24 h to avoid damage to the membrane. After modification, the membrane was rinsed in demineralized water and stored in 0.1 M NaCl at 4 °C. The membrane obtained after aza-Michael reaction is named AEM+PDA+SBMA in the following.

**2.3. Surface Modification: ATRP.** **2.3.1. Synthesis of Dopamine-BiBB.** For the chemical modification of dopamine hydrochloride, the procedure reported in the literature by Liu et al. was followed (Figure S3 in the Supporting Information).<sup>40</sup> Dopamine hydrochloride (2 g, 10.5 mmol) was dissolved in 200 mL DMF inside a three-neck round-bottom flask equipped with a condenser. Nitrogen was bubbled in the solution for 30 min. Then, 748 μL TEA (5.3 mmol) and 652 μL BiBB (5.3 mmol) were added while stirring. The

solution was stirred under nitrogen atmosphere at room temperature for 24h.

**2.3.2. Atom Transfer Radical Polymerization (ATRP).** The AEMs modified with the synthesized polydopamine-BiBB (following the same deposition process presented in section 2.2.1, Figure 1, step 1b, named in the following AEM+PDA-Br) were further modified by atom transfer radical polymerization (ATRP) to grow zwitterionic brushes on their surface with a grafting approach, similar to the process presented by Liu et al. (Figure 1, step 2b).<sup>40</sup> The same reactor design was used as for the surface modification with polydopamine (Figure S1 in the Supporting Information), with the polydopamine-BiBB layer facing the reaction solution. 5.15 g SBMA (18.4 mmol) was added to a 1:1 mixture of milli-Q water and IPA in a brown glass bottle. Then, 8 mL of a stock solution of CuCl<sub>2</sub> and TPMA (50 mg of CuCl<sub>2</sub> and 700 mg of TPMA in 100 mL of water and IPA mixture 1:1, stored under nitrogen) were added to the SBMA solution. The solution was poured in the reactor, in contact with the membrane. Nitrogen bubbles were blown in the reaction liquid for 30 min. A solution of 25 mL solution of water and IPA mixed 1:1 and 1.2 g of L-ascorbic acid was prepared. The reactor was placed on a shaking plate (60 rpm) and the ascorbic acid solution was added to start the ATRP process. Nitrogen was bubbled through the solution during the entire reaction time. After 1 h, the nitrogen flow was interrupted and the reactor was opened to stop the ATRP. After modification, the membrane was rinsed in demineralized water and stored at 4 °C. The membrane obtained after ATRP is named AEM+PDA-Br+PSBMA in the following.

**2.4. Membrane Characterizations.** The surface composition of the membranes before and after surface modification was analyzed with scan electron microscopy (SEM) and energy dispersed X-ray spectroscopy (EDS) scans. For this, the membrane samples were dried in a vacuum oven at 35 °C for 24 h. The dried membranes were twice gold coated in a JEOL JFC-1200 fine coater (Jeol (Europe) BV, The Netherlands) at 25 mA for 15 s. The samples were analyzed with SEM-EDS (JEOL JSM-6480LV, Jeol (Europe) BV, The Netherlands). SEM images were obtained with 5000× magnification, with a 6 kV accelerating voltage. The SEM images for EDS measurements were conducted at 100× magnification, applying a 12 kV accelerating voltage.

The surface composition of the membranes was characterized with attenuated total reflectance Fourier transform infrared spectroscopy (ATR-FTIR), using a Varian 3100 FTIR Excalibur Series (Agilent Technologies, U.S.A.) equipped with a Specac Golden Gate ATR insert (Specac Ltd., United Kingdom). The hydrophilicity of the membranes was evaluated with captive bubble contact angle measurements. The measurements were performed with a DataPhysics OCA 35 (DataPhysics Instruments GmbH, Germany) with a custom 3D-printed membrane holder immersed in milli-Q water. The water contact angle was obtained as the difference between 180° and the contact angle with air.

Electrical resistance was evaluated at the membrane level using a six-compartment cell and performing measurements in a through-plane fashion. Literature procedures were followed, and the solution for equilibration and testing of the membranes was 0.5 M NaCl.<sup>53,54</sup> Membrane permselectivity was evaluated according to procedures available in the literature using a two-compartment cell setup, with 0.1 and 0.5 M NaCl solutions recirculated in the two compartments.<sup>53,54</sup>

**2.5. Stack Assembly.** A cross-flow RED stack with an active area of 6.5 × 6.5 cm<sup>2</sup> was obtained from REDstack BV (The Netherlands). The end-plates housed Ti electrodes coated with 50 g/m<sup>2</sup> galvanized Pt (MAGNETO Special Anodes BV, The Netherlands). Gasket-integrated spacers with a woven netting (470 μm thickness, from Saati SpA, Italy) were obtained from Deukum GmbH (Germany). The AEMs used in this study were pristine and modified Fujifilm AEM type I (pristine, PDA, PDA-BiBB, zwitterionic monomers, and zwitterionic brushes), while the CEMs were Neosepta CMX-fg (ASTOM, Japan) sourced from Eurodia SA (France). The assembled stacks had five cell pairs (5 AEMs + 6 CEMs, with the extra CEM to seal the electrolyte compartment).

**2.6. Feedwaters.** Artificial feedwaters were used for this study. Artificial seawater contained 30 g NaCl L<sup>-1</sup> and artificial river water 1 g NaCl L<sup>-1</sup>. Both were prepared with demineralized water (produced by an Osmostar S400, Lubron Waterbehandeling BV, The Netherlands). For fouling experiments, the model compound used was sodium dodecylbenzenesulfonate (SDBS), which was added to the river water with a concentration of 100 ppm. The sequence of feedwaters used in the stack experiments was (1) artificial river and seawater without foulant (8 h), (2) clean seawater and river water containing 100 ppm of SDBS as a foulant (16 h, based on the time needed for unmodified membranes to reach a stable fouling level), and (3) again artificial river and seawater without foulant to investigate the reversibility of the fouling (3 h). SDBS was chosen as a model foulant due to its ability to produce severe fouling on short time scales, which is enabled by its negative charge, and the ability to have affinity interactions both with aromatic and aliphatic membranes, as shown by Tanaka et al.<sup>26</sup>

**2.7. Electrochemical Measurements.** Stack electrochemical measurements were performed with an Iviumstat controlled by IviumSoft (IVIUM Technologies BV, The Netherlands), while measurements with the two- and six-compartment cells were performed with an Autolab PGSTAT30 controlled by the NOVA 2.1.3 software (Metrohm Autolab BV, The Netherlands). The stack measurements were performed in a loop where a constant current density (10.5 A m<sup>-2</sup>) was alternated with a chronopotentiometric series (0–3.5–7.0–10.5–14.0 A m<sup>-2</sup>) every 15 min. This loop was running continuously during the stack experiments, with the exception of an interruption during the run with unmodified membranes, when the potentiostat disconnected from the desktop controlling it and a constant current was continuously applied to the stack. Stack open circuit voltage (OCV) was determined from the average voltage calculated on the last 10 s at 0 A m<sup>-2</sup>. The stack electrical resistance was calculated from the slope of the current–voltage curve based on the chronopotentiometric series data. Power density was calculated from the stack OCV and electrical resistance:

$$P_{\text{dens}}[\text{W m}^{-2}] = \frac{\text{OCV}^2[\text{V}^2]}{4 \times 2N_{\text{cp}}[-] \times \text{area}[\text{m}^2] \times \text{ER}[\Omega]} \quad (1)$$

where  $P_{\text{dens}}$  is the maximum gross power density, OCV is the stack open circuit voltage,  $N_{\text{cp}}$  is the number of cell pairs, area is the active area, and ER is the stack electrical resistance. This formula is derived from the assumption that maximum gross power density is attained when the external load is equal to the stack internal resistance.<sup>55</sup> The values of stack OCV, electrical resistance, and gross power density were normalized to highlight the impact of fouling on the membranes. Normalization was performed by dividing all of the values by the last values measured in the first experimental stage with clean waters and multiplying them by 100.

### 3. RESULTS AND DISCUSSION

**3.1. Membrane Characterizations.** The surface composition of the membranes before (AEM) and after modification with PDA (AEM+PDA), zwitterionic monomers (aza-Michael, AEM+PDA+SBMA), PDA-BiBB (AEM+PDA-Br), and zwitterionic brushes (ATRP, AEM+PDA-Br+PSBMA) was analyzed with SEM-EDS. Figure 2 compares the relative composition of the surface of these membranes for carbon, sulfur, and bromine.

Figure 2 clearly shows carbon as the most abundant element, both in the PDA and the aza-Michael (zwitterionic monomers) modified membranes. Simultaneously, a minor contribution of sulfur is observed for the PDA-modified membrane (AEM+PDA). Given the chemistry of the applied layer and that the unmodified membrane (Fujifilm AEM type I) is obtained from cross-linking of an acrylamide monomer carrying a quaternary ammonium group with *N,N'*-methylene bis(acrylamide) on a polyolefine-based porous support,<sup>56</sup> the presence of sulfur is

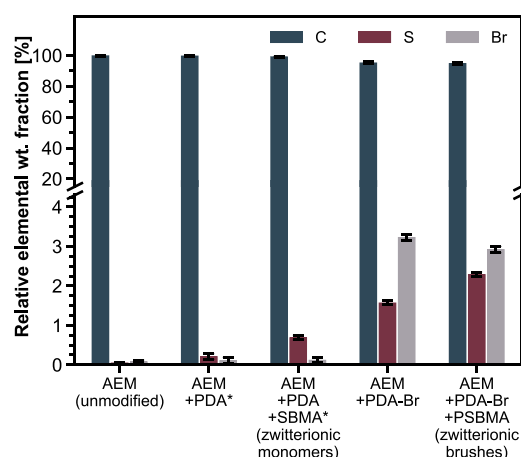


**Figure 2.** Relative weight fractions measured in the SEM-EDS spectra of the membrane surfaces for carbon (dark blue), sulfur (dark red), and bromine (gray). The error bars illustrate the measurement error as reported by the instrument. \* = samples that were equilibrated in 0.5 M NaCl prior to the analysis to reduce the amount of nonchemically bound sulfate.

not expected. The results of the SEM-EDS analysis on unmodified membranes (AEM) indeed confirm the absence of sulfur and bromine. The very small amount of S observed in the PDA-modified membrane originates from residual sulfate ions (introduced by the addition of copper sulfate pentahydrate) exchanged with chloride ions during the surface modification process and still present in the membranes in small amounts despite the equilibration in 0.5 M NaCl prior to the surface characterization. As expected, the amount of sulfur significantly increases when the PDA modified membrane is grafted with sulfobetaine monomers (via aza-Michael reaction, AEM+PDA+SBMA), due the presence of sulfonic groups in the monomers. The amount of sulfate seems low; however, this is the amount relative to a large volume of unmodified material, as the penetration depth of SEM-EDS is in the order of several micrometers. Based on data from Ruan et al. and Liu et al., the thickness of the modification layers in the present study is estimated to be in the 1–2  $\mu\text{m}$  range.<sup>39,40</sup> The results thus confirm the successful grafting of the zwitterionic monomers on the membrane surface via the aza-Michael reaction. The presence of bromine in the PDA-BiBB sample (AEM+PDA-Br) indicates that the modification of dopamine with BiBB is also successful. Again, the presence of sulfate in the PDA-BiBB sample derives from the copper sulfate pentahydrate that was used in the deposition of PDA-BiBB. Figure 2 shows that after modification with zwitterionic brushes via ATRP (AEM+PDA-Br+PSBMA), the relative fraction of sulfate increases, confirming the grafting of polysulfobetaine to the membrane surface.

In the Supporting Information, Figure S4 shows the SEM images of the membrane surface during the various stages of the surface modification. After polydopamine deposition (Figure S4b,d), the membrane surface is covered with a thin conformal PDA layer topped by PDA aggregates, consistently with the observations of Zhang et al. and Ruan et al.<sup>39,51</sup> Upon aza-Michael reaction (Figure S4c) and ATRP (Figure S4e), the aggregates are less visible and the membrane surface appears more corrugated, due to the presence of the zwitterionic layers and the exposure to solvents during the surface modification process. Additional evidence of the surface modification is

provided in Figure S5 in the Supporting Information, with the ATR-FTIR spectra of the membranes at various stages of the surface modification. The emergence of new peaks in the spectra of AEM+PDA+SBMA (Figure S5a) and AEM+PDA-Br+PSBMA (Figure S5b) at  $1726\text{ cm}^{-1}$  (carbonyl group from SBMA) and at  $1039\text{ cm}^{-1}$  (sulfonate group from SBMA) indicates the successful grafting to the membrane surface of (poly)sulfobetaine. While these characterizations determine the successful modification of the membranes, the determination of grafting density and chain length is hampered by the difficulty of determining the amount of immobilized initiator available on the surface of the membrane prior to the grafting via aza-Michael reaction and ATRP.<sup>57</sup>

Subsequently, the permselectivity and electrical resistance of the resulting membranes is determined to evaluate the effect of the membrane modifications on membrane properties and on RED performance. Figure 3 shows the membrane perm-

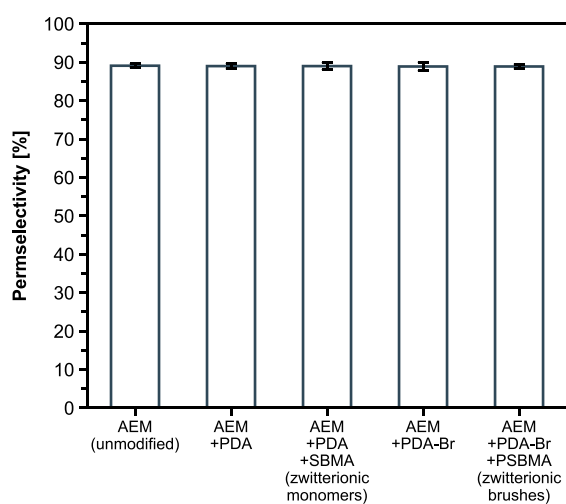


**Figure 3.** Membrane permselectivity for the membranes at different stages of surface modification. Measurement in 0.1 M/0.5 M NaCl. The error bars illustrate the minimum and maximum measured values (2 samples).

lectivity at different stages of the two membrane surface modification processes, which quantifies co-ion leakage and the ability of the membrane to generate a voltage when exposed to a salt concentration gradient across it.

Independent of the modification step, the permselectivity is high and remains constant at  $89.0 \pm 0.1\%$  for all samples. This value is slightly lower but close to those reported in the literature ( $90\%$ <sup>25</sup>). The permselectivity is not compromised because the layers are very thin due to the short deposition times. Additionally, both the PDA layer and the zwitterionic layer have a net neutral charge. Therefore, they are not expected to negatively affect the charge density of the membrane and its electrical properties. Permselectivity data for AEMs modified with PDA are scarce in literature; nevertheless, Vasselbehagh et al. reported a decreased OCV,<sup>58</sup> which is directly related to permselectivity, for AEMs modified with PDA, but in that case the modification time was much longer than in the present study (24 h vs 1 h) and the deposition temperature ( $30\text{ }^{\circ}\text{C}$  versus room temperature) was higher, with both time and temperature strongly enhancing layer formation and thus decreasing the overall membrane properties.<sup>59</sup>

Figure 4 shows the membrane electrical resistance measured at the different stages in the surface modification process.

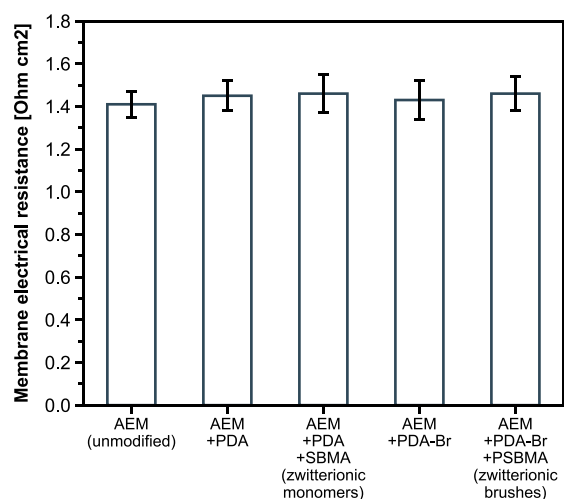


**Figure 4.** Membrane electrical resistance for the membranes at different stages of surface modification. Measurement in 0.5 M NaCl. The error bars illustrate the minimum and maximum measured values (two samples).

The average electrical resistance values seem to increase slightly upon surface modification, but the increase is very limited and within the experimental measurement error. The resistance value for the unmodified AEM is consistent with those reported in previous studies.<sup>25,60</sup> It is also confirmed by the results of Ruan et al., who did not report an increase in electrical resistance or selectivity (chloride over sulfate) as well of polydopamine modified membranes for modification times below or equal to 4.5 h. Only at 8 h deposition time a very small increase in electrical resistance and selectivity was observed in their study.<sup>38,39</sup> Additionally, Liu et al. also measured comparable permeability and salt rejection for the pristine and modified thin-film composite membranes in their study, thus reinforcing the expectation that the surface modification based on polydopamine deposition and grafting of a zwitterionic layer does not negatively impact ion transport through the membrane.<sup>40</sup> So, although an additional layer is applied on top of the membrane with every modification step (Figure 1), this layer is so thin that it does not affect the membrane properties significantly (Figures 3 and 4).

To evaluate the effect of both the zwitterionic monomers (aza-Michael) and the zwitterionic brushes (ATRP) on the hydrophilicity of the membranes, contact angle measurements of the modified membranes were determined (Figure 5). The measured air contact angles are reported in Figure S6 in the Supporting Information, together with images of the measured air bubbles.

The water contact angle value measured for the unmodified membrane is lower than what is reported in the literature, but literature values are measured with a sessile drop method on a membrane exposed to air, while the value presented in this study was measured with a captive bubble measurement method on a submerged membrane.<sup>61</sup> The introduction of both the zwitterionic monomers (aza-Michael, AEM+PDA+SBMA) and brushes (ATRP, AEM+PDA-Br+PSBMA) decreases the contact angle of the membranes with water. The decrease in contact angle means an increased hydro-

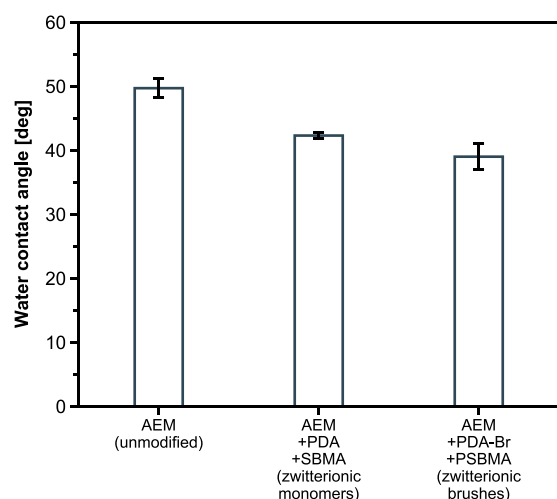


**Figure 5.** Water contact angle for the membranes at different stages of surface modification. The error bars illustrate the minimum and maximum measured values (three samples).

philicity of the modified membranes induced by the larger hydration shell of (poly)sulfobetaine.<sup>50</sup> Thanks to the larger number of zwitterionic units present in the polymeric brushes (ATRP) than in the monomers (aza-Michael), the amount of

bound water is larger for AEM+PDA-Br+PSBMA than for AEM+PDA+SBMA. Therefore, the contact angle decreases further for the zwitterionic polymeric brushes. Additionally, the decrease in contact angle confirms the successful grafting of zwitterionic monomers and brushes on the AEM surface.

Contact angle values reported in literature for other surfaces modified with (poly)sulfobetaine vary over a wide range. Liu et al. report a decrease from 75° to 20° with very short PDA deposition time and subsequent polysulfobetaine surface modification,<sup>40</sup> while Ruan et al. report a decrease from around 78° to 65° for short PDA deposition times (up to 12 h), and to 60° for longer PDA deposition times (18–24 h), accompanied by sulfobetaine monomers surface modification.<sup>39</sup> The variety of values in the literature indicates that the priming layer below the zwitterionic layer, the thickness of the zwitterionic layer, as well as the coverage of the zwitterionic layer all play a role in determining the surface wettability. Based on the work of Vasselbehagh et al., PDA layers alone can already decrease the water contact angle to values as low as 30°.<sup>35</sup> The differences in absolute value of the contact angles measured in this work and those determined by Liu et al.<sup>40</sup> and Ruan et al.<sup>39</sup> may stem from different membrane coverage, surface roughness, and PDA deposition times. Nevertheless, the hydrophilicity of the zwitterion-modified membranes (both

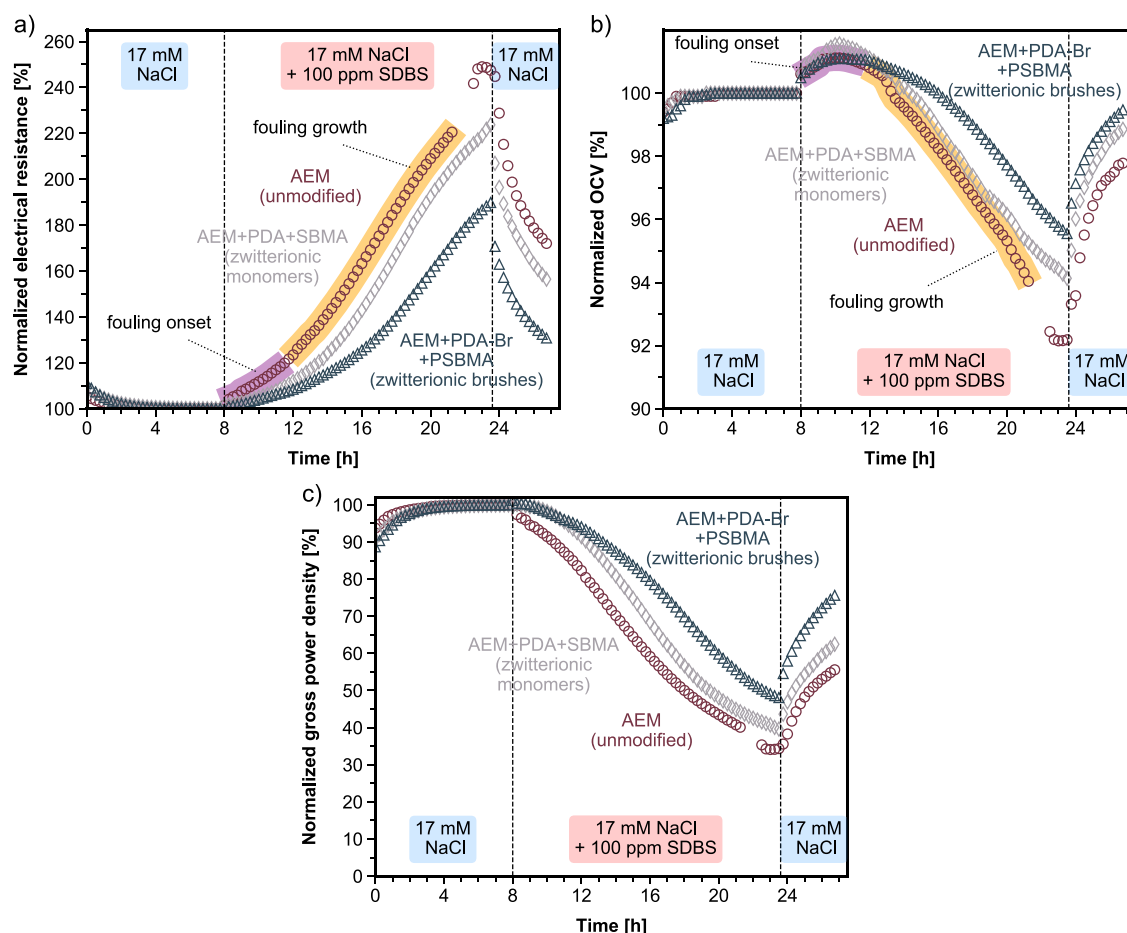


**Figure 6.** (a) Normalized electrical resistance of the RED stacks, (b) normalized OCV of the RED stacks, and (c) normalized gross power density of the RED stacks during the first 8 h with river and seawater containing only NaCl (light blue), during the fouling stage with SDBS in river water (pink), and during the cleaning stage (light blue) of the RED experiment. For the stack with unmodified membranes, the fouling onset (purple) and fouling growth (yellow) stage are highlighted in panels a and b.

with monomers and brushes) increased compared to the nonmodified counterpart.

**3.2. Stack Characterizations.** Subsequently, the fouling behavior using a frequently used model compound (SDBS) and subsequent cleaning strategies of the modified membranes in RED operation is analyzed and compared to that of their unmodified counterparts. Figure 6a shows the evolution of the normalized stack electrical resistance during the RED fouling and cleaning experiments for the stack with unmodified membranes (AEM), the stack with membranes modified with zwitterionic monomers (aza-Michael, AEM+PDA+SBMA), and the stack with membranes modified with zwitterionic brushes (ATRP, AEM+PDA-Br+PSBMA).

During the first 4 h of operation with NaCl only in the feedwaters, the stack electrical resistance decreases as the membranes equilibrate in the new solutions and air bubbles that may be trapped in the spacers are slowly expelled from the stack. After 4 h of RED operation, all stacks reached a stable stack resistance value. In our previous fouling study, electrochemical impedance spectroscopy showed that the fouling onset is associated with a decrease of the capacitive behavior of the AEM-water interface due to the nucleation of SDBS domains on the AEM surface.<sup>62</sup> These domains then grow to form a layer, which is then visible as a plateauing of the capacitive components and an increase in the nonohmic resistance of the AEM.<sup>62</sup> This evolution is now also mirrored in the behavior of the stack resistance over time in this work (indicated by the yellow and orange highlighted areas in Figure 6a). The behavior over time during the fouling stage for the stack with unmodified AEMs (Figure 6a) can be divided into three phases: fouling onset (8–12 h), growth of the fouling layer (12–22 h), and plateauing (22–23.5 h).<sup>62</sup> Both stacks with zwitterionic layers on the AEMs only show the first two phases of this process, with the fouling onset stage taking longer compared to the unmodified membranes. The fouling onset stage corresponds to the formation of SDBS domains, and the layer growth is reflected in the steady increase in stack electrical resistance in phase 2. The delayed onset of fouling for the stacks with zwitterionic monomers and brushes indicates that the growth of SDBS domains on these membranes takes more time. This is reflected in the lower rate of change of normalized stack electrical resistance over time, as illustrated in Figure S7a in the Supporting Information. The lower interaction forces between the hydrophobic model foulant and the surface of the membranes modified with zwitterionic monomers (aza-Michael) and brushes (ATRP) explain the delay in the fouling onset. The water contact angle measurements are an indication of this decreased interaction. Liu et al. performed membrane-foulant interaction force measurements, which showed a greatly reduced interaction force for membranes modified with zwitterionic brushes compared to pristine membranes.<sup>40</sup> In this respect, zwitterionic monomers are less effective than zwitterionic brushes as visible in a faster increase of the electrical resistance during the fouling growth stage, where the rate of change of the normalized stack electrical resistance for the membranes modified with zwitterionic monomers is similar to that of the unmodified membranes. This highlights the benefit of the longer zwitterionic grafts compared to the zwitterionic monomers. Upon removal of SDBS from the river water, during the cleaning stage, the three stacks exhibit similar recovery rates for the normalized stack resistance over time (Figure S7a). The reversible nature of fouling with SDBS is consistent with the

results of previous studies, where OCV and stack resistance recovered once exposed to feedwaters without the model compound.<sup>62,63</sup> After 4 h of cleaning, the stack with membranes modified with zwitterionic brushes is the closest to its original resistance, thanks to the lower extent of fouling achieved during the fouling phase.

Figure 6b shows the evolution of the normalized OCV over time during the fouling and cleaning stages of the stack experiments for the stack with unmodified membranes, the stack with membranes modified with zwitterionic monomers (aza-Michael), and the stack with membranes modified with zwitterionic brushes (ATRP). Figure S7b in the Supporting Information illustrated the rate of change of the normalized OCV over time.

During the first 2 h of operation with only NaCl in river and seawater, the stack OCVs reach an equilibrium value due to the membrane conditioning in the newly assembled stack. Surprisingly, for all membranes, the OCV increases in the first hours after the introduction of SDBS in the river water (8–10 h). Considering that 100 ppm of SDBS introduces around 10% extra sodium in the river water as well, the opposite (a reduction of the OCV upon addition of SDBS in the river water) is expected due to the corresponding decrease in sodium gradient over the CEMs. However, this is not detected. This behavior was consistently observed for all experiments.

Despite this anomaly, the evolution of the OCV closely resembles the evolution of the stack electrical resistance, albeit with fouling leading to a loss of OCV. The three stages of fouling onset, fouling growth, and plateau (only for the unmodified membranes) are identified for the OCV as well. The fouling onset is observed in the first hours of the fouling phase (8–12 h for the unmodified membranes), and it is responsible for initiating the decreasing OCV trend. The fouling growth is observed in the following hours (12–22 h for the unmodified membranes) and is represented by the steady downward trend in the normalized OCV. The OCV loss is caused by the accumulation of negatively charged SDBS on the surface of the AEM. This negatively charged layer promotes transport of positive co-ions that are normally repelled by the positively charged AEM. The increased transport of co-ions results in a reduced membrane permselectivity and in turn a reduced OCV. Equally to the membrane resistance, also here, the reduced membrane-foulant interaction forces for the membranes modified with a zwitterionic layer led to a slower accumulation of SDBS on the membrane surface, which is observed in the longer onset stage for the modified membranes, particularly in the case of zwitterionic brushes (ATRP). However, as was the case for the stack resistance, also for the OCV the membranes modified with zwitterionic monomers exhibit similar fouling rates during the fouling growth stage as the unmodified membranes (Figure S7b). After 4 h of cleaning, the stack with membranes modified with zwitterionic brushes is the closest to its original OCV, thanks to the lower degree of fouling attained at the end of the fouling growth phase.

Figure 6c shows the evolution of the stack gross power density over time during fouling and cleaning experiments for the stack with unmodified membranes, the stack with membranes modified with zwitterionic monomers (aza-Michael), and the stack with membranes modified with zwitterionic brushes (ATRP).

The trends observed for electrical resistance and OCV are now combined, and it is evident that the surface modification

with zwitterionic monomers and zwitterionic brushes is effective in reducing the power density loss upon membrane fouling with SDBS, especially when zwitterionic brushes are grafted to the membrane surface. In the fouling experiment, the stack with unmodified AEMs lost 65% of its initial gross power density, while the stack with membranes modified by zwitterionic monomers and brushes lost 60 and 52%, respectively. The reduced losses registered for modified membranes derive from their reduced interaction with the hydrophobic SDBS, resulting in a longer duration of the fouling onset stage and a slower fouling growth, especially in the case of the membranes modified with zwitterionic brushes. While zwitterionic monomers are effective in delaying the onset of fouling, as observed by Ruan et al. in their 2 h experiments,<sup>39</sup> on a longer term, the power loss very much approaches that of the unmodified membranes. Zwitterionic brushes on the other hand are more effective in not only delaying the fouling onset but also in reducing the fouling growth rate due to their more hydrophilic nature, which stem from the longer chains and the corresponding larger number of zwitterionic moieties that cover the membrane surface. For instance, after 8 h of exposure to a high concentration of model foulant, the power loss for the stack with membranes modified with zwitterionic brushes is about half of the power loss registered for the stack with unmodified membranes. It should be noted that in this study the fouling stage had the same duration for all AEMs. While this ensured consistent testing of the different membranes, a limitation of this experimental design is the inability to discern directly whether the modified membranes would reach a lower resistance plateau than the unmodified membranes. Based on the trends in the fouling rates observed in Figure S7a and S7b, it seems likely that the membranes modified with zwitterionic brushes may reach a plateau at a lower electrical resistance, while the membranes modified with zwitterionic monomers may reach a similar resistance plateau as the unmodified membranes. This hypothesis is based on the observation that the fouling rates are already decreasing for the modified membranes when the fouling stage is terminated to begin the cleaning phase of the experiment. However, an improved experimental design would be necessary to experimentally verify this hypothesis. Nevertheless, it can be observed that, in the first 8 h of the fouling phase, AEMs modified with zwitterionic brushes offer a distinct advantage compared to unmodified membranes in terms of delayed fouling onset and reduced fouling rate. Considering that the experiments were conducted at a high concentration (approximately 15 times the concentration of organic compounds found in natural feedwaters) of a model compound that induces severe fouling compared to naturally occurring substances, the benefits on antifouling resistance are expected to be even greater in real water applications with lower concentrations of organic compounds. Therefore, this research proves that in reverse electro dialysis modification of anion exchange membranes with zwitterionic brushes is a promising modification route to improve the antifouling properties of AEMs, especially in combination with periodic cleaning strategies.

#### 4. CONCLUSION

Antifouling AEMs were prepared by coating of a commercial AEM with either polydopamine followed by grafting of zwitterionic monomers on its surface or with a modified polydopamine-BiBB coating as surface initiator for ATRP with

sulfobetaine to graft zwitterionic brushes on the membrane surface. Both the polydopamine and the zwitterionic layers hardly affect the permselectivity nor the electrical resistance compared to the nonmodified membranes thanks to the thin grafting layers which is made by using short deposition and reaction times. Their membrane hydrophilicity clearly increased offering a method to better mitigate fouling. The fouling resistance for both zwitterionic monomers and zwitterionic brush membranes was improved. Unlike the zwitterionic monomers, which only delay the fouling onset, the zwitterionic brushes cause a delay in the fouling onset and also slow down the fouling layer growth. The results of this study show the potential of zwitterionic surface chemistry to prepare antifouling membranes for application in RED or other electro-membrane technologies used to process natural feedwaters.

#### ■ ASSOCIATED CONTENT

##### SI Supporting Information

The Supporting Information is available free of charge at <https://pubs.acs.org/doi/10.1021/acsami.1c02789>.

Schematic illustration of the reactor used for membrane modification; membrane modification schemes for polydopamine deposition, aza-Michael reaction, and atom transfer radical polymerization; SEM images of pristine and modified membranes; FTIR spectra of pristine and modified membranes; captive bubble contact angle values and bubble images; and plots of fouling and cleaning rates (PDF)

#### ■ AUTHOR INFORMATION

##### Corresponding Author

Kitty Nijmeijer – Membrane Materials and Processes, Department of Chemical Engineering and Chemistry, Eindhoven University of Technology, 5600 MB Eindhoven, The Netherlands; Dutch Institute for Fundamental Energy Research (DIFFER), 5600 HH Eindhoven, The Netherlands; [orcid.org/0000-0002-1431-2174](https://orcid.org/0000-0002-1431-2174); Email: [d.c.nijmeijer@tue.nl](mailto:d.c.nijmeijer@tue.nl)

##### Authors

Diego Pintossi – Wetsus, European centre of excellence for sustainable water technology, 8900 CC Leeuwarden, The Netherlands; Membrane Materials and Processes, Department of Chemical Engineering and Chemistry, Eindhoven University of Technology, 5600 MB Eindhoven, The Netherlands; [orcid.org/0000-0001-8272-7059](https://orcid.org/0000-0001-8272-7059)

Michel Saakes – Wetsus, European centre of excellence for sustainable water technology, 8900 CC Leeuwarden, The Netherlands

Zandrie Borneman – Membrane Materials and Processes, Department of Chemical Engineering and Chemistry, Eindhoven University of Technology, 5600 MB Eindhoven, The Netherlands; Dutch Institute for Fundamental Energy Research (DIFFER), 5600 HH Eindhoven, The Netherlands

Complete contact information is available at: <https://pubs.acs.org/doi/10.1021/acsami.1c02789>

##### Author Contributions

D.P.: conceptualization, methodology, investigation, visualization, and writing of the original draft. M.S.: conceptualization, supervision, writing of the review and editing, and project

administration. Z.B. and K.N.: conceptualization, supervision, and writing of the review and editing.

## Notes

The authors declare no competing financial interest.

## ACKNOWLEDGMENTS

This work was performed with the cooperation framework of Wetsus, European Centre of Excellence for Sustainable Water Technology ([www.wetsus.eu](http://www.wetsus.eu)). Wetsus is cofunded by the Dutch Ministry of Economic Affairs and Ministry of Infrastructure and Environment, the Province of Fryslân, and the Northern Netherlands Provinces. This project has also received funding from the European Union's Horizon 2020 research and innovation program under the Marie Skłodowska-Curie Grant Agreement No 665874. Open access publication was enabled by an ACS Read + Publish Agreement stipulated with VSNU, the consortium of Dutch universities. The authors would like to thank the participants of the research theme "Blue Energy" for their input and suggestions and their financial support. The authors are also grateful to C. de Carvalho Esteves from the Physical Chemistry laboratory of the Chemical Engineering and Chemistry department of Eindhoven University of Technology for her input and suggestions. Finally, the authors express their gratitude to C. Weijers and D. Scheepers from the Membrane Materials and Processes group at Eindhoven University of Technology for their support in carrying out membrane surface characterizations.

## REFERENCES

- (1) Post, J. W.; Veerman, J.; Hamelers, H. V. M.; Euverink, G. J. W.; Metz, S. J.; Nijmeijer, K.; Buisman, C. J. N. Salinity-Gradient Power: Evaluation of Pressure-Retarded Osmosis and Reverse Electrodialysis. *J. Membr. Sci.* **2007**, *288* (1–2), 218–230.
- (2) Giacalone, F.; Vassallo, F.; Griffin, L.; Ferrari, M. C.; Micale, G.; Scargiali, F.; Tamburini, A.; Cipollina, A. Thermolytic Reverse Electrodialysis Heat Engine: Model Development, Integration and Performance Analysis. *Energy Convers. Manage.* **2019**, *189*, 1–13.
- (3) Giacalone, F.; Vassallo, F.; Scargiali, F.; Tamburini, A.; Cipollina, A.; Micale, G. The First Operating Thermolytic Reverse Electrodialysis Heat Engine. *J. Membr. Sci.* **2020**, *595*, 117522.
- (4) Tedesco, M.; Brauns, E.; Cipollina, A.; Micale, G.; Modica, P.; Russo, G.; Helsen, J. Reverse Electrodialysis with Saline Waters and Concentrated Brines: A Laboratory Investigation towards Technology Scale-Up. *J. Membr. Sci.* **2015**, *492*, 9–20.
- (5) Tedesco, M.; Cipollina, A.; Tamburini, A.; Micale, G. Towards 1 KW Power Production in a Reverse Electrodialysis Pilot Plant with Saline Waters and Concentrated Brines. *J. Membr. Sci.* **2017**, *522*, 226–236.
- (6) Post, J. W.; Hamelers, H. V. M.; Buisman, C. J. N. Energy Recovery from Controlled Mixing Salt and Fresh Water with a Reverse Electrodialysis System. *Environ. Sci. Technol.* **2008**, *42* (15), 5785–5790.
- (7) Alvarez-Silva, O. A.; Osorio, A. F.; Winter, C. Practical Global Salinity Gradient Energy Potential. *Renewable Sustainable Energy Rev.* **2016**, *60*, 1387–1395.
- (8) Lacey, R. E. Energy by Reverse Electrodialysis. *Ocean Eng.* **1980**, *7* (1), 1–47.
- (9) Logan, B. E.; Elimelech, M. Membrane-Based Processes for Sustainable Power Generation Using Water. *Nature* **2012**, *488* (7411), 313–319.
- (10) Galama, A. H.; Post, J. W.; Hamelers, H. V. M.; Nikonenko, V. V.; Biesheuvel, P. M. On the Origin of the Membrane Potential Arising across Densely Charged Ion Exchange Membranes: How Well Does the Teorell-Meyer-Sievers Theory Work? *Journal of Membrane Science and Research* **2016**, *2* (3), 128–140.
- (11) Veerman, J.; Saakes, M.; Metz, S. J.; Harmsen, G. J. Reverse Electrodialysis: Evaluation of Suitable Electrode Systems. *J. Appl. Electrochem.* **2010**, *40* (8), 1461–1474.
- (12) Moreno, J.; Grasman, S.; van Engelen, R.; Nijmeijer, K. Upscaling Reverse Electrodialysis. *Environ. Sci. Technol.* **2018**, *52* (18), 10856–10863.
- (13) Post, J. W.; Goeting, C. H.; Valk, J.; Goinga, S.; Veerman, J.; Hamelers, H. V. M.; Hack, P. J. F. M. Towards Implementation of Reverse Electrodialysis for Power Generation from Salinity Gradients. *Desalin. Water Treat.* **2010**, *16* (1–3), 182–193.
- (14) Vermaas, D. A.; Kunteng, D.; Saakes, M.; Nijmeijer, K. Fouling in Reverse Electrodialysis under Natural Conditions. *Water Res.* **2013**, *47* (3), 1289–1298.
- (15) Daniilidis, A.; Herber, R.; Vermaas, D. A. Upscale Potential and Financial Feasibility of a Reverse Electrodialysis Power Plant. *Appl. Energy* **2014**, *119*, 257–265.
- (16) Güler, E.; Nijmeijer, K. Reverse Electrodialysis for Salinity Gradient Power Generation: Challenges and Future Perspectives. *Journal of Membrane Science and Research* **2018**, *4* (3), 108–110.
- (17) Vermaas, D. A.; Saakes, M.; Nijmeijer, K. Early Detection of Preferential Channeling in Reverse Electrodialysis. *Electrochim. Acta* **2014**, *117*, 9–17.
- (18) Kingsbury, R. S.; Liu, F.; Zhu, S.; Boggs, C.; Armstrong, M. D.; Call, D. F.; Coronell, O. Impact of Natural Organic Matter and Inorganic Solutes on Energy Recovery from Five Real Salinity Gradients Using Reverse Electrodialysis. *J. Membr. Sci.* **2017**, *541*, 621–632.
- (19) Guo, H.; Xiao, L.; Yu, S.; Yang, H.; Hu, J.; Liu, G.; Tang, Y. Analysis of Anion Exchange Membrane Fouling Mechanism Caused by Anion Polyacrylamide in Electrodialysis. *Desalination* **2014**, *346*, 46–53.
- (20) Lee, H.-J.; Kim, D. H.; Cho, J.; Moon, S.-H. Characterization of Anion Exchange Membranes with Natural Organic Matter (NOM) during Electrodialysis. *Desalination* **2003**, *151* (1), 43–52.
- (21) Lee, H.-J.; Hong, M.-K.; Han, S.-D.; Shim, J.; Moon, S.-H. Analysis of Fouling Potential in the Electrodialysis Process in the Presence of an Anionic Surfactant Foulant. *J. Membr. Sci.* **2008**, *325* (2), 719–726.
- (22) Lee, H.-J.; Hong, M.-K.; Han, S.-D.; Cho, S.-H.; Moon, S.-H. Fouling of an Anion Exchange Membrane in the Electrodialysis Desalination Process in the Presence of Organic Fouling. *Desalination* **2009**, *238* (1–3), 60–69.
- (23) Lindstrand, V.; Sundström, G.; Jönsson, A.-S. Fouling of Electrodialysis Membranes by Organic Substances. *Desalination* **2000**, *128* (1), 91–102.
- (24) Lindstrand, V.; Jönsson, A.-S.; Sundström, G. Organic Fouling of Electrodialysis Membranes with and without Applied Voltage. *Desalination* **2000**, *130* (1), 73–84.
- (25) Rijnaarts, T.; Moreno, J.; Saakes, M.; de Vos, W. M.; Nijmeijer, K. Role of Anion Exchange Membrane Fouling in Reverse Electrodialysis Using Natural Feed Waters. *Colloids Surf., A* **2019**, *560*, 198–204.
- (26) Tanaka, N.; Nagase, M.; Higa, M. Organic Fouling Behavior of Commercially Available Hydrocarbon-Based Anion-Exchange Membranes by Various Organic-Fouling Substances. *Desalination* **2012**, *296*, 81–86.
- (27) Moreno, J.; de Hart, N.; Saakes, M.; Nijmeijer, K. CO<sub>2</sub>-saturated Water as Two-Phase Flow for Fouling Control in Reverse Electrodialysis. *Water Res.* **2017**, *125*, 23–31.
- (28) Vermaas, D. A.; Kunteng, D.; Veerman, J.; Saakes, M.; Nijmeijer, K. Periodic Feedwater Reversal and Air Sparging as Antifouling Strategies in Reverse Electrodialysis. *Environ. Sci. Technol.* **2014**, *48* (5), 3065–3073.
- (29) Kotoka, F.; Merino-Garcia, I.; Velizarov, S. Surface Modifications of Anion Exchange Membranes for an Improved Reverse Electrodialysis Process Performance: A Review. *Membranes* **2020**, *10* (8), 160.

- (30) Güler, E.; van Baak, W.; Saakes, M.; Nijmeijer, K. Monovalent-Ion-Selective Membranes for Reverse Electrodialysis. *J. Membr. Sci.* **2014**, *455*, 254–270.
- (31) Banerjee, I.; Pangule, R. C.; Kane, R. S. Antifouling Coatings: Recent Developments in the Design of Surfaces That Prevent Fouling by Proteins, Bacteria, and Marine Organisms. *Adv. Mater.* **2011**, *23* (6), 690–718.
- (32) Kochkodan, V.; Hilal, N. A Comprehensive Review on Surface Modified Polymer Membranes for Biofouling Mitigation. *Desalination* **2015**, *356*, 187–207.
- (33) Park, J.-S.; Lee, H.-J.; Choi, S.-J.; Geckeler, K. E.; Cho, J.; Moon, S.-H. Fouling Mitigation of Anion Exchange Membrane by Zeta Potential Control. *J. Colloid Interface Sci.* **2003**, *259* (2), 293–300.
- (34) Hao, L.; Liao, J.; Jiang, Y.; Zhu, J.; Li, J.; Zhao, Y.; van der Bruggen, B.; Sotto, A.; Shen, J. Sandwich-like Structure Modified Anion Exchange Membrane with Enhanced Monovalent Selectivity and Fouling Resistant. *J. Membr. Sci.* **2018**, *556*, 98–106.
- (35) Vasselbehagh, M.; Karkhanечи, H.; Mulyati, S.; Takagi, R.; Matsuyama, H. Improved Antifouling of Anion-Exchange Membrane by Polydopamine Coating in Electrodialysis Process. *Desalination* **2014**, *332* (1), 126–133.
- (36) Vasselbehagh, M.; Karkhanечи, H.; Takagi, R.; Matsuyama, H. Effect of Polydopamine Coating and Direct Electric Current Application on Anti-Biofouling Properties of Anion Exchange Membranes in Electrodialysis. *J. Membr. Sci.* **2016**, *515*, 98–108.
- (37) Li, Y.; Shi, S.; Cao, H.; Zhao, Z.; Su, C.; Wen, H. Improvement of the Antifouling Performance and Stability of an Anion Exchange Membrane by Surface Modification with Graphene Oxide (GO) and Polydopamine (PDA). *J. Membr. Sci.* **2018**, *566*, 44–53.
- (38) Ruan, H.; Zheng, Z.; Pan, J.; Gao, C.; van der Bruggen, B.; Shen, J. Mussel-Inspired Sulfonated Polydopamine Coating on Anion Exchange Membrane for Improving Permselectivity and Anti-Fouling Property. *J. Membr. Sci.* **2018**, *550*, 427–435.
- (39) Ruan, H.; Liao, J.; Tan, R.; Pan, J.; Sotto, A.; Gao, C.; Shen, J. Dual Functional Layers Modified Anion Exchange Membranes with Improved Fouling Resistant for Electrodialysis. *Adv. Mater. Interfaces* **2018**, *5* (20), 1800909.
- (40) Liu, C.; Lee, J.; Ma, J.; Elimelech, M. Antifouling Thin-Film Composite Membranes by Controlled Architecture of Zwitterionic Polymer Brush Layer. *Environ. Sci. Technol.* **2017**, *51* (4), 2161–2169.
- (41) Liu, Q.; Li, W.; Wang, H.; Liu, L. A Facile Method of Using Sulfobetaine-Containing Copolymers for Biofouling Resistance. *J. Appl. Polym. Sci.* **2014**, *131* (18), 9432–9440.
- (42) Wang, J.; Qiu, M.; He, C. A Zwitterionic Polymer/PES Membrane for Enhanced Antifouling Performance and Promoting Hemocompatibility. *J. Membr. Sci.* **2020**, *606*, 118119.
- (43) Jiang, S.; Cao, Z. Ultralow-Fouling, Functionalizable, and Hydrolyzable Zwitterionic Materials and Their Derivatives for Biological Applications. *Adv. Mater.* **2010**, *22* (9), 920–932.
- (44) Chiang, Y.-C.; Chang, Y.; Chuang, C.-J.; Ruaan, R.-C. A Facile Zwitterionization in the Interfacial Modification of Low Bio-Fouling Nanofiltration Membranes. *J. Membr. Sci.* **2012**, *389*, 76–82.
- (45) Ji, Y.-L.; An, Q.-F.; Zhao, Q.; Sun, W.-D.; Lee, K.-R.; Chen, H.-L.; Gao, C.-J. Novel Composite Nanofiltration Membranes Containing Zwitterions with High Permeate Flux and Improved Anti-Fouling Performance. *J. Membr. Sci.* **2012**, *390–391*, 243–253.
- (46) Davenport, D. M.; Lee, J.; Elimelech, M. Efficacy of Antifouling Modification of Ultrafiltration Membranes by Grafting Zwitterionic Polymer Brushes. *Sep. Purif. Technol.* **2017**, *189*, 389–398.
- (47) Sun, Q.; Su, Y.; Ma, X.; Wang, Y.; Jiang, Z. Improved Antifouling Property of Zwitterionic Ultrafiltration Membrane Composed of Acrylonitrile and Sulfobetaine Copolymer. *J. Membr. Sci.* **2006**, *285* (1–2), 299–305.
- (48) Nunes, S. P. Can Fouling in Membranes Be Ever Defeated? *Curr. Opin. Chem. Eng.* **2020**, *28*, 90–95.
- (49) Virga, E.; Žvab, K.; de Vos, W. M. Fouling of Nanofiltration Membranes Based on Polyelectrolyte Multilayers: The Effect of a Zwitterionic Final Layer. *J. Membr. Sci.* **2021**, *620*, 118793.
- (50) He, M.; Gao, K.; Zhou, L.; Jiao, Z.; Wu, M.; Cao, J.; You, X.; Cai, Z.; Su, Y.; Jiang, Z. Zwitterionic Materials for Antifouling Membrane Surface Construction. *Acta Biomater.* **2016**, *40*, 142–152.
- (51) Zhang, C.; Ou, Y.; Lei, W.-X.; Wan, L.-S.; Ji, J.; Xu, Z.-K. CuSO<sub>4</sub>/H<sub>2</sub>O<sub>2</sub>-Induced Rapid Deposition of Polydopamine Coatings with High Uniformity and Enhanced Stability. *Angew. Chem., Int. Ed.* **2016**, *55* (9), 3054–3057.
- (52) Mather, B. D.; Viswanathan, K.; Miller, K. M.; Long, T. E. Michael Addition Reactions in Macromolecular Design for Emerging Technologies. *Prog. Polym. Sci.* **2006**, *31* (5), 487–531.
- (53) Güler, E.; Elizen, R.; Vermaas, D. A.; Saakes, M.; Nijmeijer, K. Performance-Determining Membrane Properties in Reverse Electrodialysis. *J. Membr. Sci.* **2013**, *446*, 266–276.
- (54) Dlugolecki, P.; Nijmeijer, K.; Metz, S.; Wessling, M. Current Status of Ion Exchange Membranes for Power Generation from Salinity Gradients. *J. Membr. Sci.* **2008**, *319* (1–2), 214–222.
- (55) Veerman, J.; Post, J. W.; Saakes, M.; Metz, S. J.; Harmsen, G. J. Reducing Power Losses Caused by Ionic Shortcut Currents in Reverse Electrodialysis Stacks by a Validated Model. *J. Membr. Sci.* **2008**, *310* (1–2), 418–430.
- (56) van Engelen, J. Composite Membranes. Patent number WO2013/014420A1, 2013.
- (57) Mastan, E.; Xi, L.; Zhu, S. Factors Affecting Grafting Density in Surface-Initiated ATRP: A Simulation Study. *Macromol. Theory Simul.* **2016**, *25* (3), 220–228.
- (58) Vasselbehagh, M.; Karkhanечи, H.; Takagi, R.; Matsuyama, H. Biofouling Phenomena on Anion Exchange Membranes under the Reverse Electrodialysis Process. *J. Membr. Sci.* **2017**, *530*, 232–239.
- (59) Oymaci, P.; Nijmeijer, K.; Borneman, Z. Development of Polydopamine Forward Osmosis Membranes with Low Reverse Salt Flux. *Membranes* **2020**, *10* (5), 10050094 DOI: 10.3390/membranes10050094.
- (60) Pintossi, D.; Chen, C.-L.; Saakes, M.; Nijmeijer, K.; Borneman, Z. Influence of Sulfate on Anion Exchange Membranes in Reverse Electrodialysis. *npj Clean Water* **2020**, *3* (1), 29.
- (61) Zhao, Y.; Liu, H.; Tang, K.; Jin, Y.; Pan, J.; der Bruggen, B. V.; Shen, J.; Gao, C. Mimicking the Cell Membrane: Bio-Inspired Simultaneous Functions with Monovalent Anion Selectivity and Antifouling Properties of Anion Exchange Membrane. *Sci. Rep.* **2016**, *6* (1), 37285.
- (62) Pintossi, D.; Saakes, M.; Borneman, Z.; Nijmeijer, K. Electrochemical Impedance Spectroscopy of a Reverse Electrodialysis Stack: A New Approach to Monitoring Fouling and Cleaning. *J. Power Sources* **2019**, *444*, 227302.
- (63) Bodner, E. J.; Saakes, M.; Sleutels, T.; Buisman, C. J. N.; Hamelers, H. V. M. The RED Fouling Monitor: A Novel Tool for Fouling Analysis. *J. Membr. Sci.* **2019**, *570–571*, 294–302.